Heavy Quark Production at HERA

Ian C. Brock – *Version 1.0*[*]

Physikalisches Institut, Universität Bonn, Bonn, Germany

Abstract

Heavy flavour production is one of the key components of the HERA II physics programme. While most of the results presented use leptons or the reconstruction of charmed mesons to identify heavy flavour production, both the H1 and ZEUS experiments now have working microvertex detectors that are being used more and more. In this talk I will summarise a selection of the recent results obtained by the two collaborations.

1. Introduction

The study of heavy flavour production at HERA provides an important test of perturbative Quantum Chromodynamics (pQCD) and also valuable information for the measurements to be made at the LHC. I will discuss a small selection of the many measurements of heavy flavour production that have been made at HERA, concentrating on the more recent results.

HERA running started in 1992 and the accelerator stopped running at the end of June 2007. HERA collided 27.5 GeV electrons or positrons[1] with 920 GeV (820 GeV until the end of 1997) protons, giving a centre-of-mass energy of 318 GeV. A long shutdown in 2000 and 2001 was used to upgrade the machine and the detectors, with the aim of increasing the luminosity by about a factor of 4. The period up to 2000 is usually called HERA I and after 2001 HERA II. By the end of the running both of the colliding beam experiments, H1 and ZEUS, had collected about 0.5 fb^{-1} of data.

Several kinematic variables are used to characterise the ep scattering process:

- Q^2, the negative squared four-momentum exchanged at the electron or positron vertex;
- x, the Bjorken scaling variable;
- y, the inelasticity;
- W, the invariant mass of the hadronic final state.

The measurements are usually separated into the deep inelastic scattering (DIS), $Q^2 \gtrsim 1\,\text{GeV}^2$, or photoproduction, $Q^2 \lesssim 1\,\text{GeV}^2$, regimes, depending on whether the scattered electron is detected in the in the main calorimeter or not.

The main production mechanism for heavy quarks is the so-called Boson Gluon Fusion (BGF) process which is illustrated in Figure 1. In practice higher order contributions also have to be taken into account. The photon can fluctuate into a $q\bar{q}$ pair and one of the quarks then participates in the hard interaction (resolved photoproduction); or in so-called excitation the scattering from charm or beauty can take place with intrinsic charm or beauty inside the proton or photon. Monte Carlo models usually include these process in addition to the direct boson-gluon fusion. These higher order processes are also sometimes referred to collectively as non-direct.

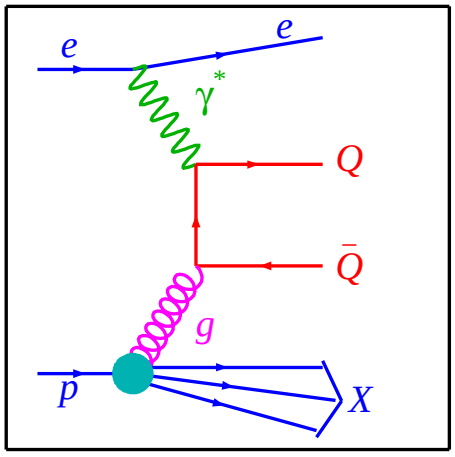

Figure 1: Feynman diagram of the boson gluon fusion process.

Next-to-leading oder (NLO) QCD calculations exist for heavy quark production at HERA. These are implemented for photoproduction in the FMNR programme[1, 2] and for DIS in the HVQDIS programme[3]. The programmes include simple independent fragmentation of the b or c quark, but on their own are not able to give predictions for correlations between final-state particles. The FMNR programme has been interfaced[4] to the Pythia Monte Carlo and its predictions have been used for studies of dimuon final states.

Most heavy flavour measurements rely on the central tracking detectors and are helped significantly by the presence of a microvertex detector. H1 had such a detector for some of the HERA I running, while both ZEUS and H1 had such detectors

[*]On behalf of the H1 and ZEUS Collaborations

Email addresses: brock@physik.uni-bonn.de (Ian C. Brock – *Version 1.0*)

[1]Hereafter unless explicitly stated both electrons and positrons are referred to as electrons.

for the HERA II running period.

Several different methods have been used by the collaborations to identify the production of heavy quarks. Each of them has its advantages and disadvantages and often cover different kinematic ranges. Traditionally the identification of D^* mesons and semileptonic decays have been used most often. With the advent of microvertex detectors lifetime information is being used more and more often. This works best for events with high energy jets, while tagging with semileptonic decays to electrons or double tags enables one to go to lower transverse momenta.

2. D^* Production

The H1 collaboration have made a series of measurements of D^* production both in the photoproduction[5] ($96\,\mathrm{pb}^{-1}$ of data taken in 2006 and 2007) and the DIS[6] ($347\,\mathrm{pb}^{-1}$ from the HERA II running period) regimes. For these measurements they make use of their new Fast Track Trigger, which enables events with D^* candidates to be selected early in the trigger chain. In both photoproduction and DIS clear signals are seen as illustrated in Figure 2. The kinematic cuts are indicated in the figures.

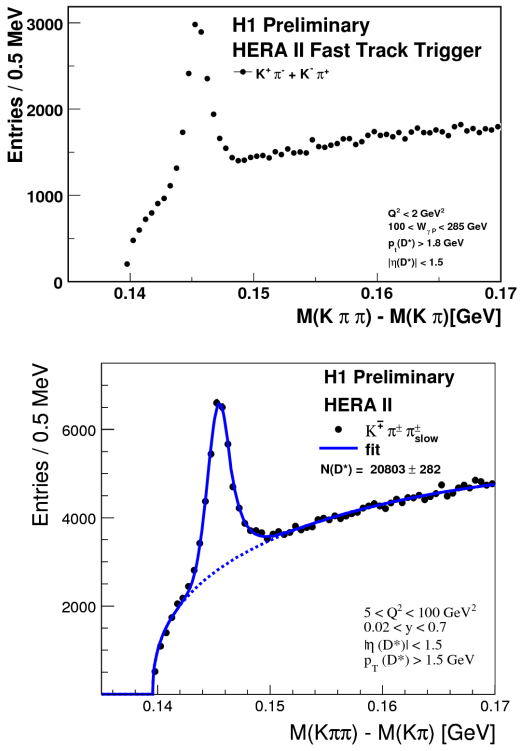

Figure 2: $\Delta M = m(K\pi\pi) - m(K\pi)$ distributions for the photoproduction (top) and DIS (bottom) samples. The points show the data, the curves in the lower figure, the results of a fit to the distribution. The dotted line shows the background shape. The kinematic cuts are indicated.

Differential cross-sections as a function of a wide range of variables have been determined. The cross-section as a function of Q^2 is shown in Figure 3. The measurements are compared to the predictions of the HVQDIS programme using two different

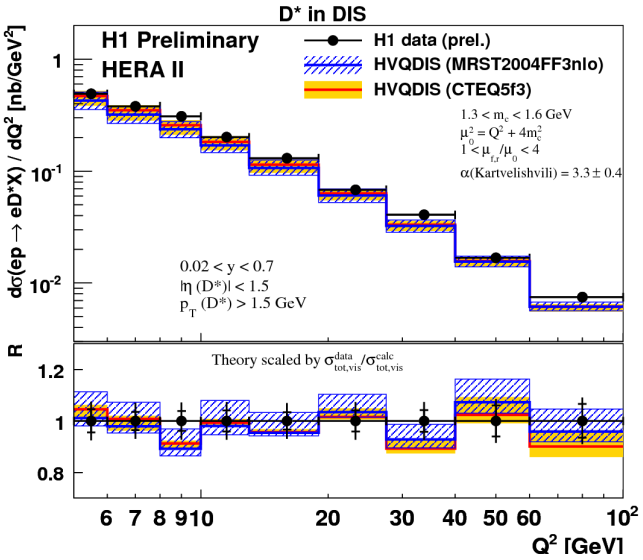

Figure 3: D^* production cross-section as a function of Q^2. The data (points) are compared to NLO QCD predictions with two different PDFs. The lower plot shows the NLO QCD prediction scaled by the ratio of the data to NLO QCD visible cross-sections. The range of variation of the quark mass and factorisation and renormalisation scales are indicated in the figure.

Parton Distribution Functions (PDF). The different PDFs show a very similar behaviour as a function of Q^2.

In contrast the cross-section as a function of the pseudorapidity, η, shows a clear dependence (see Figure 4), demonstrating the sensitivity of charm production to the gluon structure function.

Making the same comparison for photoproduction one sees that the prediction underestimates the data in the forward direction. (Figure 5). Comparing the data to Monte Carlo predictions, the Cascade generator, which is based upon k_T-factorisation, is able to provide a better description of the data in DIS (see Figure 6). However, in photoproduction Pythia, using the massless scheme for the generation of the heavy quarks, provides the best description of the data, while Cascade and Pythia in the massive mode both undershoot the data in the forward direction.

3. Beauty in Photoproduction

The ZEUS collaboration recently reported two new measurements of b-quark production in photoproduction. The first measurement uses semileptonic decays to muons[7] to identify heavy quark decays, while the second uses electrons[8]. Dijet events are selected by requiring at least two jets with $|\eta| < 2.5$ and a transverse momentum (muon measurement) or energy (electron measurement) greater than 7 GeV for the highest transverse energy and 6 GeV for the 2nd highest transverse energy jet.

The first measurement uses $124\,\mathrm{pb}^{-1}$ of data collected in 2005 and requires a well identified muon with $p_T > 2.5\,\mathrm{GeV}$ and $-1.6 < \eta < 2.3$. The microvertex detector is used to measure the impact parameter (δ) of identified muons. This is com-

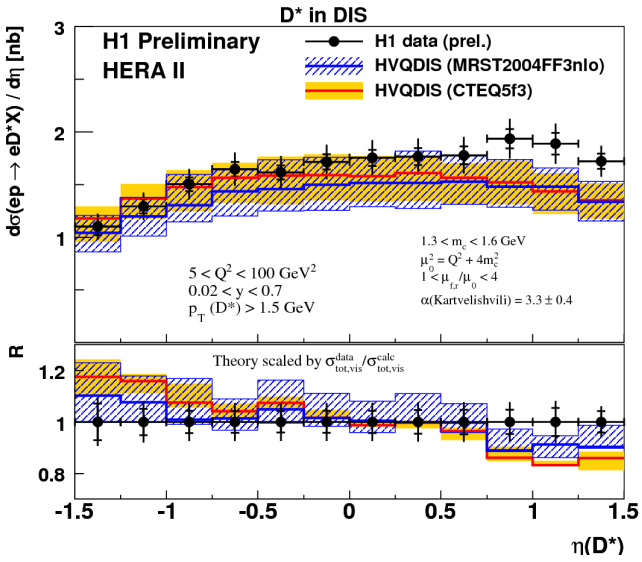

Figure 4: D^* production cross-section in DIS as a function of $\eta(D^*)$ compared to NLO QCD predictions. For further details see the caption of Figure 3.

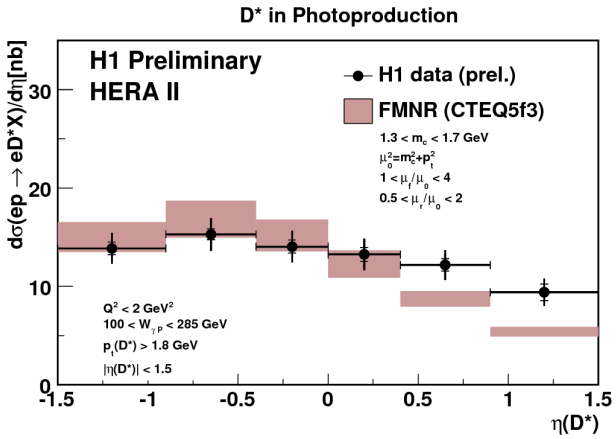

Figure 5: D^* production cross-section in photoproduction as a function of $\eta(D^*)$ compared to the NLO QCD prediction. The band shows the uncertainty in the prediction. The range of variation of the quark mass and factorisation and renormalisation scales are indicated in the figure.

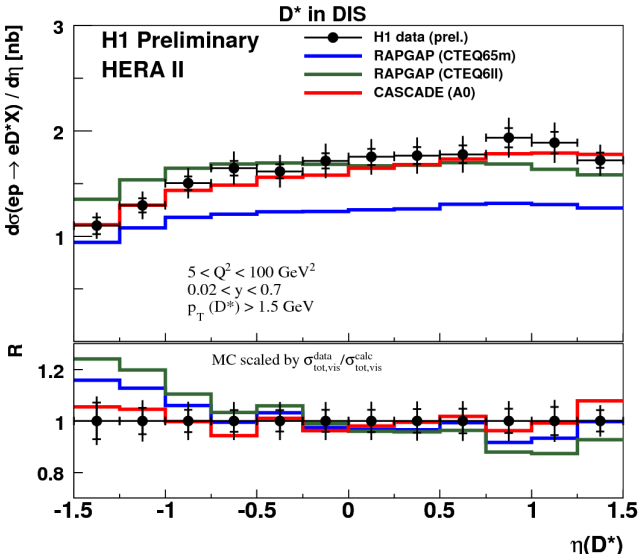

Figure 6: D^* production cross-section in DIS as a function of $\eta(D^*)$. The data are compared to the different Monte Carlo generators as indicated in the figure.

bined with the transverse momentum of the muon with respect to the jet axis (p_T^{rel}) to separate b-quark events from background. The cross-sections as a function of the transverse momentum and pseudorapidity of the muon are shown in Figures 7 and 8.

Both the charm and beauty contributions are left free in the fit. The figures also show the results of an analysis using the HERA I data[9], which only used p_T^{rel} for separation. For this earlier analysis the charm content was fixed. Good agreement between the analyses is seen. The predictions of the NLO QCD prediction are also in good agreement with the data.

The second measurement identifies electrons from the semileptonic decays of heavy quarks using an integrated luminosity of 120 pb^{-1} collected during the HERA I running period. Electron identification uses the measurement of the specific energy loss, dE/dx, in the Central Tracking Detector, CTD, the fraction of the energy deposited in the electromagnetic calorimeter as well as the ratio of the energy deposited in the calorimeter to the momentum measured in the tracking detectors. Semileptonic decays are separated from background using p_T^{rel} and the azimuthal angle between the electron direction and the missing transverse momentum vector, $\Delta\phi$. As illustrated in Figure 9, p_T^{rel} can separate b-quark from c-quark decays, while $\Delta\phi$ separates semileptonic decays from background.

The variables are combined using a likelihood ratio method, which is optimised for the identification of electron from semileptonic b-quark decays. The distribution of the likelihood ratio is shown in Figure 10. The distribution is fit using the expected distributions for beauty, charm and background to determine the fractions of events from each source. The fit provides a very good description of the data.

The visible ep cross sections (at hadron level) for b-quark and c-quark production and the subsequent semileptonic decay to an electron with $p_T^e > 0.9\,\mathrm{GeV}$ in the range $|\eta^e| < 1.5$ in photoproduction events with $Q^2 < 1\,\mathrm{GeV}^2$ and $0.2 < y < 0.8$

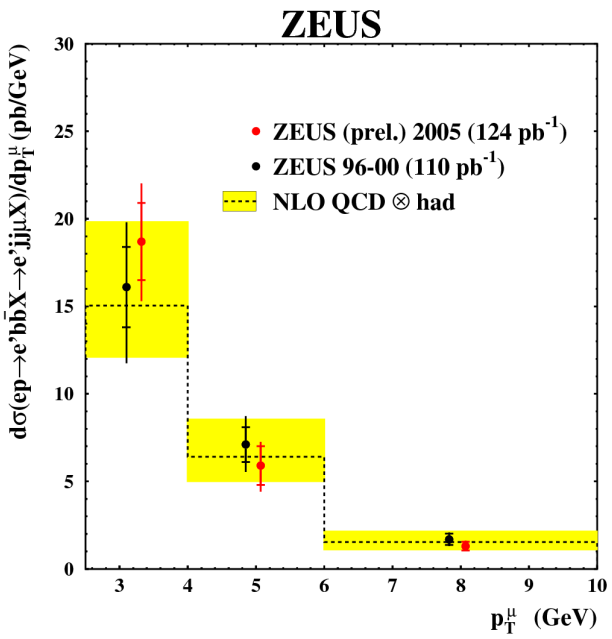

Figure 7: *b*-quark production cross-section in dijet photoproduction as a function of the transverse momentum of the muon. The measurement is compared to an earlier ZEUS publication[9] and the NLO QCD prediction. The uncertainty on the prediction is indicated by the band.

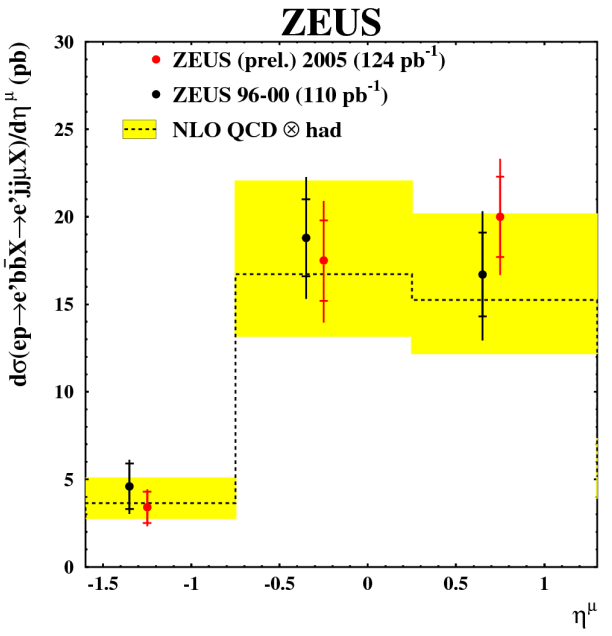

Figure 8: *b*-quark production cross-section in dijet photoproduction as a function of the pseudorapidity of the muon. The measurement is compared to an earlier ZEUS publication[9] and the NLO QCD prediction. The uncertainty on the prediction is indicated by the band.

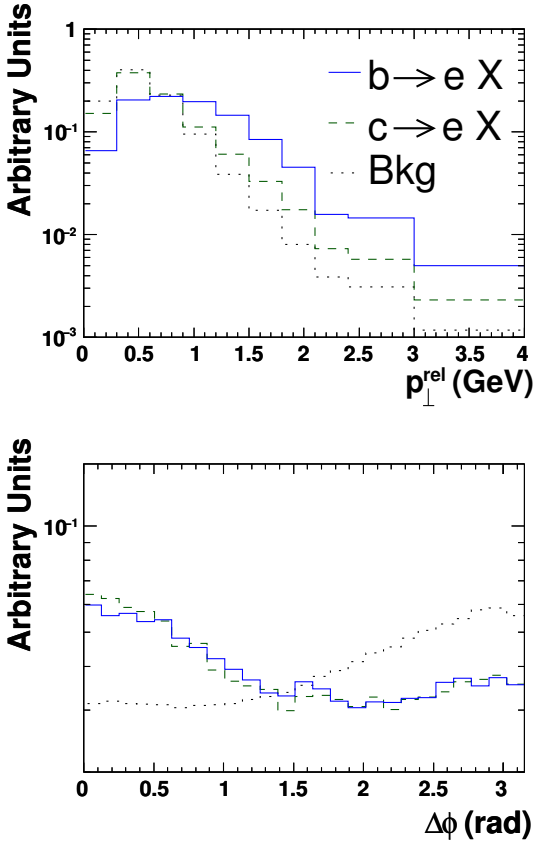

Figure 9: Variables used to separate semileptonic heavy quark decays from background. The solid line shows the distribution for electrons from semileptonic *b*-quark decays, the dashed line for *c*-quark decays and the dotted line the background (Bkg).

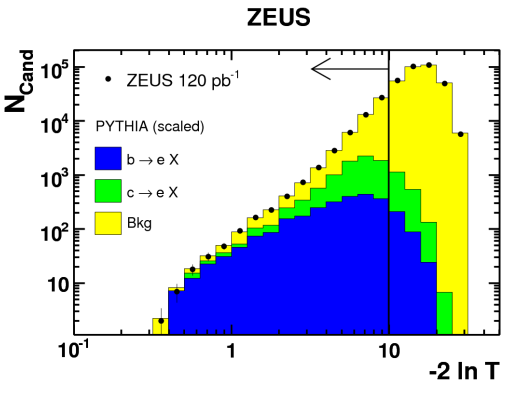

Figure 10: The distribution of the likelihood ratio for electron candidates, $N_{\rm cand}$, in data compared to the Monte Carlo expectation after the scaling the predictions to best fit the data. The arrow indicates the region included in the fit ($-2 \ln T < 10$). The shaded areas show the fitted contributions from *b* quarks, *c* quarks and background as denoted in the figure.

and at least two jets with $E_T > 7(6)\,\text{GeV}$, $|\eta| < 2.5$ were determined separately for $\sqrt{s} = 300\,\text{GeV}$ and $\sqrt{s} = 318\,\text{GeV}$. For the complete data set (96 – 00) the cross-sections evaluated at $\sqrt{s} = 318\,\text{GeV}$ are

$$\sigma_b^{\text{vis}} = \left(125 \pm 11(\text{stat.})^{+10}_{-11}(\text{syst.})\right)\text{pb},$$
$$\sigma_c^{\text{vis}} = \left(278 \pm 33(\text{stat.})^{+48}_{-24}(\text{syst.})\right)\text{pb}.$$

These cross-sections are in agreement with the corresponding NLO QCD predictions:

$$\sigma_b^{\text{NLO}} = \left(88^{+22}_{-13}\right)\text{pb},$$
$$\sigma_c^{\text{NLO}} = \left(380^{+48}_{-24}\right)\text{pb}.$$

The cross-sections as a function of the transverse momentum and pseudorapidity of the electron are shown in Figure 11. Good agreement with the NLO QCD prediction is seen. The data also agree well with the PYTHIA prediction scaled by a factor of 1.75 for b-quark production and 1.28 for c-quark production.

4. Beauty Correlations

The identification of both heavy-quark decays in an event has several advantages: the background is reduced substantially and the kinematic range accessible is larger. The disadvantage is a significant reduction of statistics. If both b-quark jets can be identified, dijet correlations can be directly measured which probe next-to-leading order effects. The ZEUS collaboration used the HERA I data sample to select dijet events ($E_T > 8\,\text{GeV}$) with two identified muons[10]. Separating the samples according to the relative charge of the muons as well as their invariant mass allows much of the background to be evaluated directly from the data. The distribution of the invariant mass of the two muons for unlike sign muons shown is Figure 12. In the low mass sample a clear J/ψ peak is visible. In the high mass sample, the contribution from $b\bar{b}$ is large.

The extracted cross-section is shown in Figure 13. It is compared with the NLO QCD prediction as well as with a leading order Monte Carlo. Given the limited statistics it is not possible to say whether the NLO calculation provides a better description of the data.

5. $F_2^{b\bar{b}}$ and $F_2^{c\bar{c}}$

The H1 collaboration have used the impact parameter significance to determine $F_2^{b\bar{b}}$ and $F_2^{c\bar{c}}$ for $12\,\text{GeV}^2 < Q^2 < 650\,\text{GeV}^2$ and $0.0002 < x < 0.032$ using $56\,\text{pb}^{-1}$ of data taken in 2006[11]. The distribution of the impact parameter in the transverse plane is shown in Figure 14.

In order to separate beauty and charm from background the two tracks with the most significant impact parameters (S_1 and S_2 respectively) are selected, rejecting events where the signs of the impact parameters differ. The significance is defined as $\delta/\sigma(\delta)$, where $\sigma(\delta)$ is the error on δ. Events with one good track

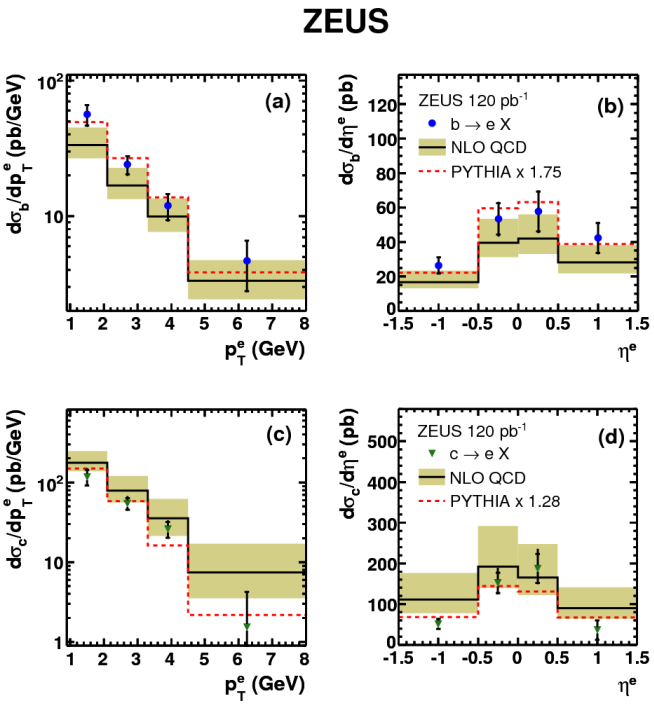

Figure 11: Differential cross sections as a function of a), c) the transverse momentum and b), d) the pseudorapidity of the electrons. Plots a) and b) are for b-quark production while c) and d) are for c-quark production. The measurements are shown as points. The inner error bar shows the statistical uncertainty and the outer error bar shows the statistical and systematic uncertainties added in quadrature. The solid line shows the NLO QCD prediction after hadronisation corrections, with the theoretical uncertainties indicated by the band; the dashed line shows the scaled prediction from PYTHIA.

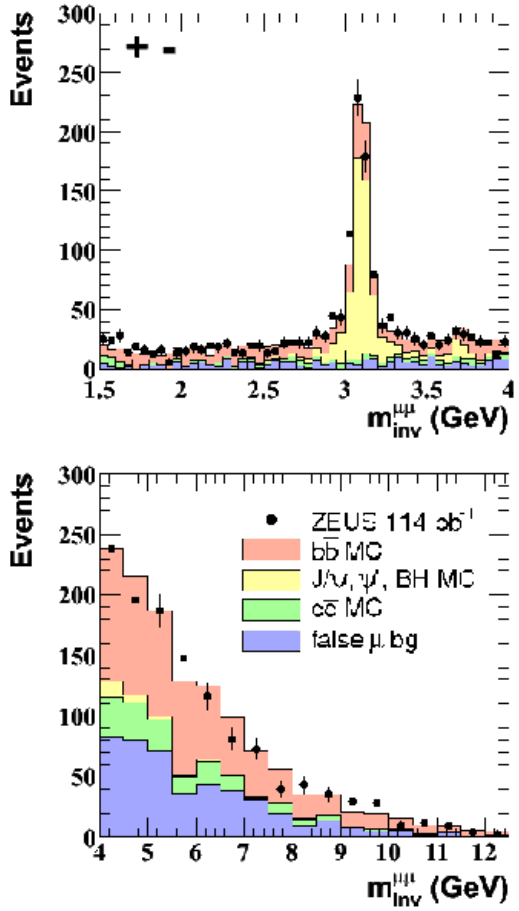

Figure 12: The dimuon invariant mass for unlike sign muons in dijet events. The upper plots shows events with $m_{\mu\mu} < 4\,\text{GeV}$ while the lower one is for $m_{\mu\mu} > 4\,\text{GeV}$. The shaded areas show the different contributions as indicated in the figure.

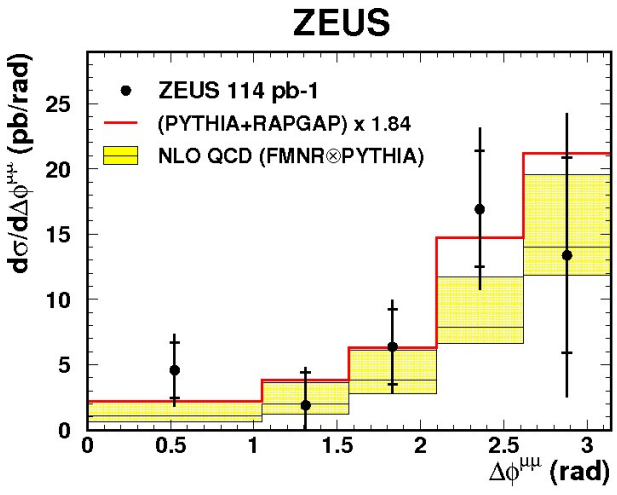

Figure 13: The dimuon cross-section as a function of the azimuthal angle between the muons in dijet events. The data (points) are compared to the NLO QCD prediction calculated using the FMNRxPYTHIA interface as well as to the RAPGAP prediction scaled by a factor of 1.84. The inner error bar shows the statistical uncertainty and the outer error bar shows the statistical and systematic uncertainties added in quadrature.

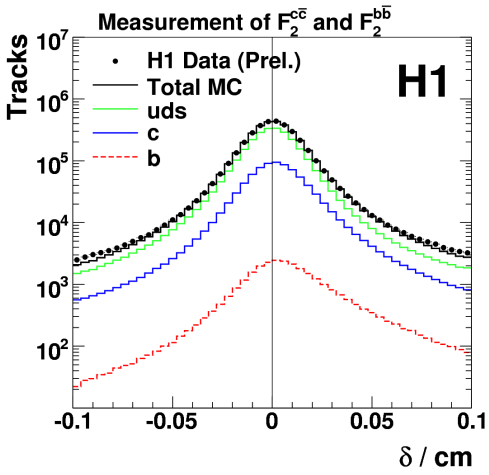

Figure 14: Distribution of the signed impact parameter for the data (points) and the contributions from b, c and light quarks, evaluated using Monte Carlo events.

are used to make the S_1 distribution; all other events are used for the S_2 distribution.

The contents of the negative significance bins are subtracted from the corresponding positive significance bins. This yields the distribution of S_2 shown in Figure 15. The charm contribu-

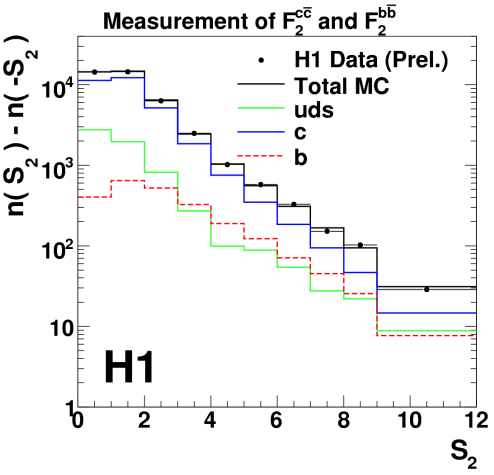

Figure 15: Distribution of the second highest significance and the contributions from b, c and light quarks, evaluated using Monte Carlo events.

tion dominates the distribution. At high significance the beauty contribution becomes larger. The data are split into bins in Q^2 and x and the contributions of beauty and charm are determined separately in each bin using a least squares simultaneous fit to the S_1 and S_2 distributions. The overall normalisation is determined by also including in the fit the total number of inclusive events without any cut on the impact parameter significance. The results of the fit in each $x - Q^2$ bin are converted to a "reduced cross-section" using

$$\tilde{\sigma}^{c\bar{c}}(x, Q^2) = \frac{d^2\sigma^{c\bar{c}}}{dx\,dQ^2} \frac{xQ^4}{2\pi\alpha^2(1 + (1-y)^2)}\,. \qquad (1)$$

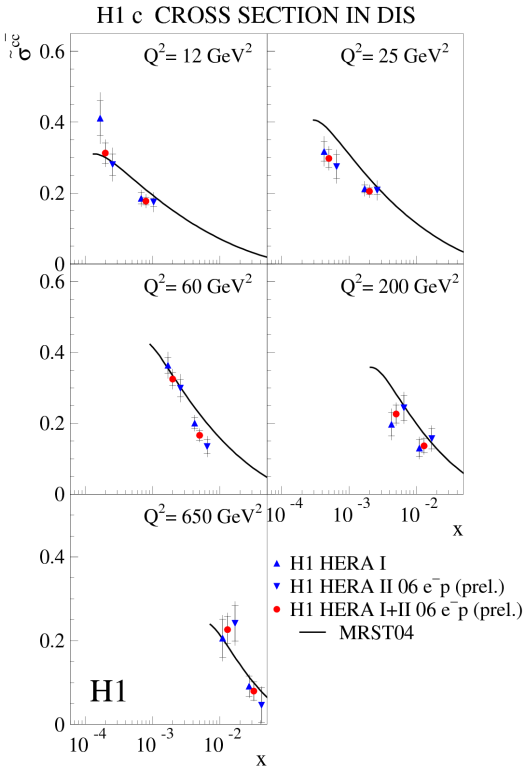

Figure 16: The reduced cross-section for $c\bar{c}$ production in different Q^2 bins as a function of x. The inner errors bars show the statistical uncertainty, the outer error bars represent the statistical and systematic uncertainties added in quadrature. The measurements are compared with those from HERA I and the averaged data are also shown. The measurements are compared to the MRST04 prediction.

The reduced cross section for $c\bar{c}$ production as a function of x in different Q^2 bins is shown in Figure 16. Measurements made with the HERA I data in the same kinematic range are also shown in the figure. The results are in good agreement with each other and can be combined, taking into account the correlated systematic errors. The prediction using the Variable Flavour Number Scheme (VFNS) in the MRST04 PDF agrees well with the data.

From the reduced cross-section $F_2^{c\bar{c}}$ can be extracted:

$$\tilde{\sigma}^{c\bar{c}}(x, Q^2) = F_2^{c\bar{c}} - \frac{y^2}{(1 + (1 - y)^2)} F_L^{c\bar{c}}, \qquad (2)$$

The correction due to the longitudinal structure function, $F_L^{c\bar{c}}$, is small. The same formulae with c replaced by b can be used to extract $\tilde{\sigma}^{b\bar{b}}$ and $F_2^{b\bar{b}}$. The measurements of $F_2^{c\bar{c}}$ and $F_2^{b\bar{b}}$ are shown in Figures 17 and 18, respectively. The rapid increase in $F_2^{c\bar{c}}$ as a function of Q^2 at low x is clearly visible. The $F_2^{b\bar{b}}$ measurements are consistent with the same trend, but are less precise.

6. Conclusions

The many HERA measurements of beauty production in photoproduction are compared in Figure 19. The measurements

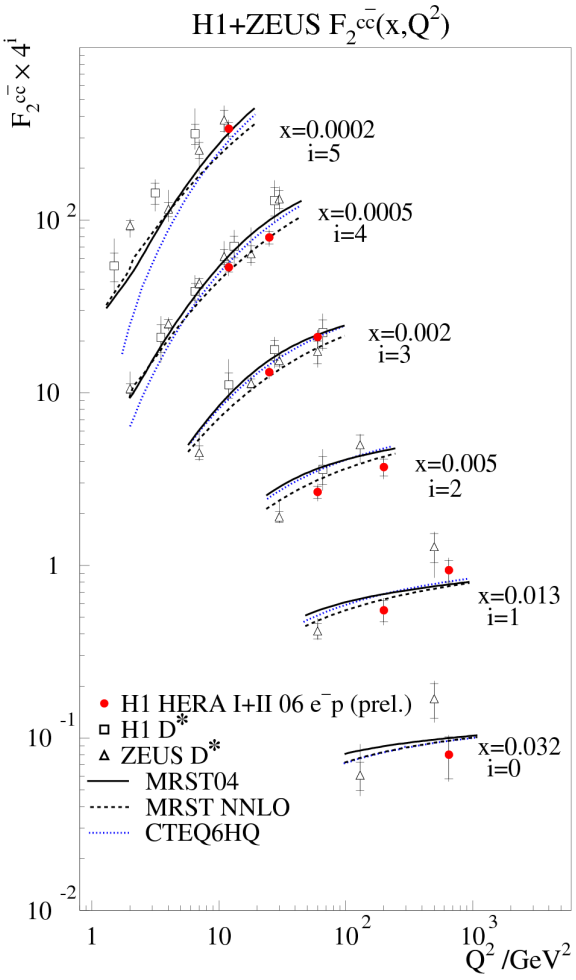

Figure 17: $F_2^{c\bar{c}}$ as a function of Q^2 for different x ranges. Also shown are measurements from the H1 and ZEUS collaborations using D^* mesons to identify the charm quarks. The inner errors bars show the statistical uncertainty, the outer error bars represent the statistical and systematic uncertainties added in quadrature.

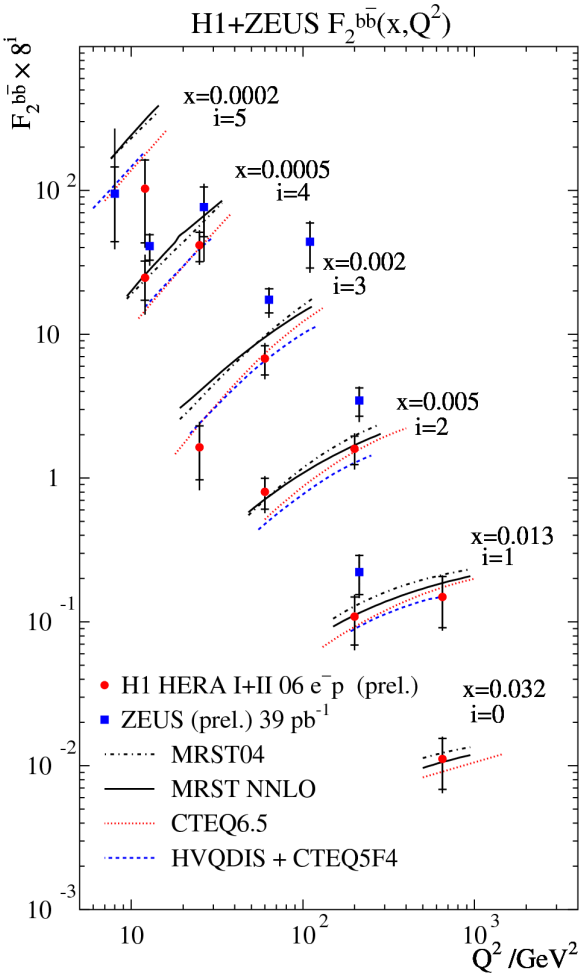

Figure 18: $F_2^{b\bar{b}}$ as a function of Q^2 for different x ranges. Also shown is a preliminary measurement from the ZEUS collaboration using the data from 2004. The inner errors bars show the statistical uncertainty, the outer error bars represent the statistical and systematic uncertainties added in quadrature.

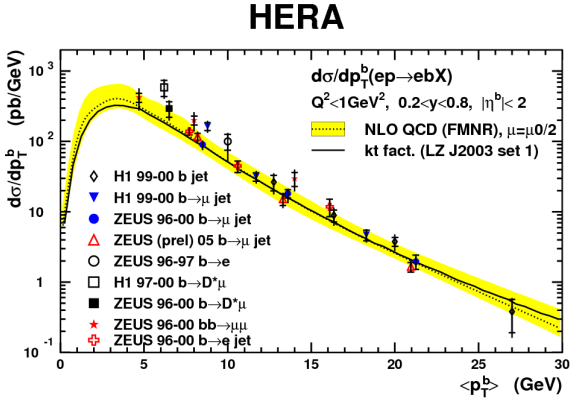

Figure 19: Differential cross section for b-quark production as a function of transverse momentum, p_T^b, compared to the results of previous ZEUS measurements as indicated in the figure. The measurements are shown as points. The inner error bar shows the statistical uncertainty and the outer error bar shows the statistical and systematic uncertainties added in quadrature. The solid line shows the NLO QCD prediction from the FMNR program with the theoretical uncertainty shown as the shaded band.

presented here agree well with the previous values, giving a consistent picture of b-quark production in ep collisions in the photoproduction regime, and are well reproduced by the NLO QCD calculations. For all the measurements leading order Monte Carlo predictions also describe well the shapes of the distributions.

There is a tendency for the measurements to overshoot the predictions in the forward direction. Comparing charm quark predictions using different PDFs shows that the cross-section is, as expected, sensitive to the gluon PDF.

In the near future a number of final HERA I measurements will be published. With the HERA II data the kinematic range of the measurements can be extended and a combination of different tagging methods should increase the precision of the measurements. The improved HERA II forward tracking will allow much improved studies of heavy quark production in the forward direction.

Acknowledgements

It is a pleasure to thanks the organisers for making this an informative and enjoyable conference. I would like to thank Cristi Diaconu, Achim Geiser, Markus Jüngst, Monica Turcato, André Schöning and Matthew Wing for their help in preparing this talk.

References

[1] S. Frixione, M. Mangano, P. Nason, G. Ridolfi, Heavy-quark correlations in photon-hadron collisions, Nucl. Phys. B 412 (1994) 225.

[2] S. Frixione, M. Mangano, P. Nason, G. Ridolfi, Heavy-quark production, Adv. Ser. Direct. High Energy Phys. 15 (1998) 609. arXiv:hep-ph/9702287.

[3] B. W. Harris, J. Smith, Charm quark and $D^{*\pm}$ cross sections in deeply inelastic scattering at DESY HERA, Phys. Rev. D 57 (1998) 2806.

[4] A. Geiser, A. E. Nuncio Quiroz, The FMNRxPYTHIA interface for heavy quark production at HERA, J. Phys. Conf. Ser. 110 (2008) 022036. arXiv:0707.1632, doi:10.1088/1742-6596/110/2/022036.

[5] H1 Coll., F. D. Aaron, et al., Measurement of D^* meson production in photoproduction, prepared XVI International Workshop on Deep-Inelastic Scattering, DIS2008 (Apr. 2008).

[6] H1 Coll., F. D. Aaron, et al., D^* production at low Q^2 with the H1 detector, prepared XVI International Workshop on Deep-Inelastic Scattering, DIS2008 (Apr. 2008).

[7] ZEUS Coll., S. Chekanov, et al., Measurement of beauty photoproduction at HERA II, prepared for EPS 2007 conference (Jul. 2007).

[8] ZEUS Coll., S. Chekanov, et al., Beauty photoproduction using decays into electrons at HERA, Accepted by Phys. Rev. Dhttp://arxiv.org/abs/0805.4390 arXiv:0805.4390.

[9] ZEUS Coll., S. Chekanov, et al., Bottom photoproduction measured using decays into muons in dijet events in ep collisions at $\sqrt{s}$ = 318 GeV, Phys. Rev. D 70 (2004) 012008. arXiv:hep-ex/0312057.

[10] I. Bloch, Measurement of beauty production from dimuon events at HERA / ZEUS, Ph.D. thesis, Hamburg University (2005).

[11] H1 Coll., F. D. Aaron, et al., Measurement of $F_2^{c\bar{c}}$ and $F_2^{b\bar{b}}$ using the H1 vertex detector at HERA, prepared for 23rd International Symposium on Lepton-Photon Interactions at High Eneergy, LP2007 (Aug. 2007).